

Autonomous Obstacle Avoidance Control Strategy for Intelligent Vehicle Based on Lateral and Longitudinal Safety Distance Model*

Fuhao Xia

School of Advanced Manufacturing Engineering
Chongqing University of Posts and Telecommunications
Chongqing, China
s202101020@stu.cqupt.edu.cn

Sijun Li

School of Advanced Manufacturing Engineering
Chongqing University of Posts and Telecommunications
Chongqing, China
s192101005@stu.cqupt.edu.cn

Haiqing Li*

School of Advanced Manufacturing Engineering
Chongqing University of Posts and Telecommunications
Chongqing, China
lihq@cqupt.edu.cn

Abstract—Obstacle avoidance decision is an important basis for path planning and the basic logic for establishing obstacle avoidance control methods. For the problems of the existing safety distance model's insufficient adaptability and single obstacle avoidance mode in complex traffic environments, an obstacle avoidance decision method based on lateral and longitudinal safety distance models is proposed. After establishing the longitudinal safety distance model which considers the road adhesion coefficient, the lane change safety distance interval model, the vehicle obstacle avoidance logic is designed. To constrain the vehicle obstacle avoidance deceleration, the peak adhesion coefficient is estimated by the Burckhardt tire model. The simulation results indicated that the method can effectively avoid vehicle collisions and enhanced the safety of driving.

Keywords—*Lateral and Longitudinal Safety Distance, obstacle avoidance strategy, Peak adhesion coefficient, Active Safety Technology*

I. INTRODUCTION

Obstacle avoidance strategy is an important topic in the field of automotive assisted driving technology. The safety distance model is an effective method for evaluating the safety status of driving based on information that identifies the movement of surrounding vehicles. Assisted driving systems based on safety distance models, including adaptive cruise control (ACC) and automatic emergency braking (AEB), are very effective in preventing collisions caused by accidental emergency braking or driver misuse [1-3].

Most of the ACC and AEB systems are developed based on three classical safety distance models, such as the safety distance model based on headway time [4], the safety distance model based on the braking process [5], and the safety distance model based on the driver model [6]. These studies illustrate how the two vehicles maintain their spacing in the longitudinal direction. However, the vehicle's obstacle avoidance mode can only consider braking obstacle avoidance and cannot achieve lane change operation, which is hardly adaptable to the complex road environment.

To solve the problem that the safety distance model fails to consider the lateral lane change characteristics of vehicles. Tian [7] proposed a lateral active obstacle avoidance system based on fuzzy and sliding mode control. The system constructed a lane-changing obstacle avoidance logic

through a safe distance. When the vehicle encounters an obstacle, the controller calculated the optimal trajectory and controlled the yaw angle to avoid the obstacle by changing lanes. Wu [8] proposed an LC strategy with a real-time obstacle avoidance function. For the two obstacle avoidance conditions of the current lane and the target lane vehicles, a two-level judgment condition and control mode matrix were constructed to control the vehicle to achieve lateral obstacle avoidance. However, the above two methods only consider the motion characteristics of the vehicle in a single direction, and can only control the vehicle for a single mode of obstacle avoidance. The reliability of the single-mode safe distance model is difficult to guarantee when the traffic environment is complex.

This paper discusses how to combine longitudinal safety distances and lateral safety distances and make the safety distance model adaptable to complex traffic environments, and also considers the influence of road surface adhesion coefficient on braking. A lateral and longitudinal safety distance model for estimating the road adhesion coefficient is proposed. Following establishment of an obstacle avoidance decision system by using the model, the effectiveness and adaptability of the method are verified by simulation in Carsim/Matlab.

II. SAFETY DISTANCE MODEL

A. Longitudinal Safety Distance Model

Based on the information obtained through the sensors such as obstacle vehicle speed and vehicle spacing, the decision system calculates the safety distance between the vehicle and the surrounding vehicles, which can determine the current danger condition of the vehicle. The braking distance of the vehicle is the crucial indicator of the safety distance. The braking distance can be calculated by the following equation:

$$S_d = (t_{lag} + \frac{t_d}{2}) \times v_i + \frac{v_i^2}{2a_{\mu_{max}}} \quad (1)$$

where t_{lag} is the driver reaction time, t_d is the brake effective time, v_i is the initial speed of the vehicle and $a_{\mu_{max}}$ is the maximum deceleration.

In addition to the braking distance, a certain distance

should be reserved in the safety distance model to prevent vehicle collisions, which is the distance d between the two vehicles when the rear vehicle stops.

The specific longitudinal safety distance of a vehicle is determined by the motion state of the vehicle in front of it. In the safety distance model, the safety distances are subdivided according to three different states of motion of the vehicle in front:

$$\begin{cases} S_{b1} = (t_{lag} + \frac{t_d}{2}) \times v_i + \frac{v_i^2}{2a_{\mu\max}} + d \\ S_{b2} = (v_i - v_f) \times t_{lag} + \frac{(v_i - v_f)^2}{2a_{\mu\max}} + \frac{(v_i + v_f)t_d}{2} + d \\ S_{b3} = v_i \times t_{lag} + \frac{(v_i - v_f)t_d}{2} + \frac{v_i^2 - v_f^2}{2a_{\mu\max}} + d \end{cases} \quad (2)$$

where S_{b1} , S_{b2} and S_{b3} are the safety distance correspond to the preceding vehicle stopped, the preceding vehicle moving at a constant speed or accelerating, and the preceding vehicle moving at a deceleration, respectively, and v_f is the speed of the preceding vehicle.

B. Lateral safety Distance Model

1) Minimum Lane Change Time

The lane change operation, while the vehicle is moving, can effectively improve the traffic flow and increase the efficiency of using the road. The steering angle change rate of the vehicle in an emergency is large, the steering angle change time is short, and the lane change process can be approximated as a fixed speed lane change process. In the process of lane change at a fixed speed, the minimum time for lane change can be obtained from the length of the vehicle lane change path and the vehicle speed. The lane change trajectory established in this paper can be regarded as consisting of two arcs, AB and BC. As shown in Fig. 1, point A is the center point of the vehicle head, point B is the intersection point of the vehicle head and the road line, and point C is the center point of the vehicle head after the lane change is completed. The vehicle lane change time model is calculated by the following equation:

$$\begin{cases} R = \frac{L}{\sin \sigma} \\ \theta = \arccos \frac{(1 + \cos \sigma)R - W}{2R} - \sigma \\ T_{cl} = \frac{2\pi R(2\theta + \sigma)}{360v_i} \end{cases} \quad (3)$$

where R is the steering radius, L is the arc AB, σ is the front wheel steering angle, θ is the angle of the circle corresponding to the arc AB, W is the lane width, and T_{cl} is the minimum lane change time.

2) Safe Distance Model for Lateral Lane Change

The main vehicle is affected by the motion state and spatial location of vehicles in the surrounding lanes when changing lanes. A new lateral lane change safety distance model based on the minimum lane change time is established in this paper to ensure the safety of the vehicle lane change

process. At the moment of collision with the preceding vehicle, the lateral displacement of the main vehicle changing lane satisfies the following equation:

$$y(T_c) \geq \frac{W_1}{2} + \frac{W_2}{2} + d_0 \quad (4)$$

where T_c is the moment of rear-end, W_1 is the vehicle width, W_2 is the preceding vehicle width, and d_0 is the minimum lateral distance maintained between vehicles.

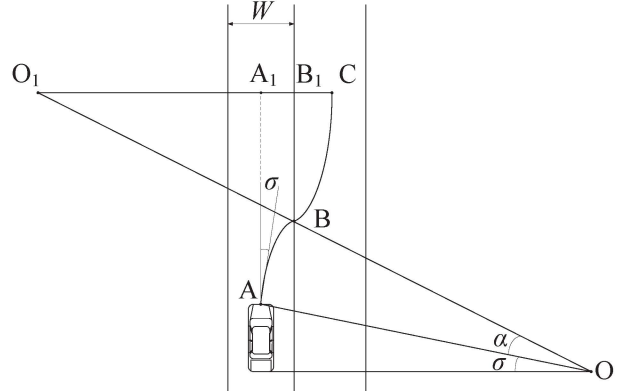


Fig. 1. Vehicle lane change process

Safe distance between the main vehicle and preceding vehicle can be expressed as:

$$\frac{2\pi R\sigma \times v_y}{360v_i} \geq \frac{W_1}{2} + \frac{W_2}{2} + d_0 \quad (5)$$

The distance to the preceding vehicle in the target lane after the lane change and the distance to the rear vehicle in the target lane after the lane change can be represented respectively as:

$$D_1 = S_{lf} - (v_i - v_{lf}) \times T_{cl} + \frac{a_{lf} \times T_{cl}^2}{2} \quad (6)$$

$$D_2 = S_{lb} - (v_i - v_{lb}) \times T_{cl} - \frac{a_{lb} \times T_{cl}^2}{2} \quad (7)$$

where v_{lb} is the velocity of the rear-vehicle, a_{lb} is the acceleration of the rear-vehicle, v_{lf} is the velocity of the preceding vehicle, and a_{lf} is the acceleration of the preceding vehicle, S_{lf} is the longitudinal distance between self-vehicle and the preceding vehicle of surrounding lane, and S_{lb} is the longitudinal distance between self-vehicle and the rear-vehicle of surrounding lane. The parameters that describe the spatiotemporal characteristics of the vehicle are represented in Fig. 2.

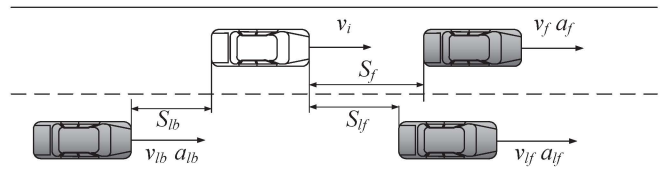


Fig. 2. Safety distance model of lane change

To avoid collisions, vehicles that have changed lanes

should maintain a longitudinal safety distance from the vehicles in the surrounding lanes.

$$D_1 > S_b \& D_2 > S_b \quad (8)$$

where S_b is one of the three longitudinal safety distances, which is selected by the operating state of the preceding vehicle and rear-vehicle after the lane change.

III. ACTIVE OBSTACLE AVOIDANCE DECISION-MAKING

A. Estimated road adhesion coefficient

The deceleration of the vehicle is closely related to the road adhesion coefficient. To determine the minimum safe distance, an estimate of the peak road adhesion coefficient is required to determine the maximum braking deceleration. The Effect-Based method estimates the pavement adhesion coefficient based on the whole-vehicle response caused by pavement changes, which is characterized by low cost, wide applicability, and strong robustness [9]. In this paper, the Effect-Based method [10] is used to estimate the road adhesion coefficient based on the state parameters of the vehicle obtained from the vehicle dynamics response characteristics.

The road adhesion coefficient is defined by the equation:

$$\mu = \frac{F_x}{F_z} \quad (9)$$

The ground longitudinal reaction force F_x of the tire in equation (9) is calculated from the results of the tire force analysis and the information of the onboard sensors. Assuming a straight driving surface, a quarter-car model is used for force analysis.

$$J\alpha = T - T_f - F_x R_t \quad (10)$$

The adhesion coefficient of the current driving road can be calculated from equation (9) and equation (10) :

$$\mu = \frac{T - T_f - J\alpha}{F_z R_t} \quad (11)$$

where J is the tire rotational inertia, α is the tire rotational angular acceleration, T is the tire moment, T_f is the friction moment between the tire and the road, R_t is the tire radius, and F_z is the ground normal reaction force.

When the vehicle enters emergency conditions, the vehicle needs to brake at the maximum deceleration speed of the current driving surface to obtain the maximum ground braking force.

The eigenvalues of the similarity between the driving surface and the Burckhardt tire model on a typical road surface are used to estimate the peak adhesion coefficient of the current driving surface [11], which is defined as:

$$\mu_{\max} = k_1 \mu_{1\max} + k_2 \mu_{2\max} \quad (12)$$

$$\begin{cases} k_1 = \frac{\mu_1 - \mu}{\mu_1 - \mu_2} \\ k_2 = \frac{\mu - \mu_2}{\mu_1 - \mu_2} \end{cases} \quad (13)$$

where $\mu_{1\max}$ and $\mu_{2\max}$ are the peak adhesion coefficients of the two types of pavements in the Burckhardt tire model, μ_1 and μ_2 are the adhesion coefficients of the two types, k_1 and k_2 are similar eigenvalues of the relation curve between road adhesion coefficient and slip rate in the Burckhardt tire model.

The parameters in equation (12) and equation (13) satisfy the relationship as follows:

$$k_1 + k_2 = 1 \quad (14)$$

$$\mu_1 > \mu > \mu_2 \quad (15)$$

The adhesion coefficient μ of the current road surface can be calculated from equation (10). The slip rate of the road surface can be estimated according to the definition of wheel slip rates[12]. The slip rates during driving and braking are defined as:

$$s = \frac{v_i - R\omega}{v_i} \quad (16)$$

$$s = \frac{R\omega - v_i}{R\omega} \quad (17)$$

where ω is the tire rotational angular velocity.

Based on the relation curve between road adhesion coefficient and slip rate in the Burckhardt tire model, the peak adhesion coefficient can be calculated. The model for estimating the peak adhesion coefficient of road is shown in Fig. 3.

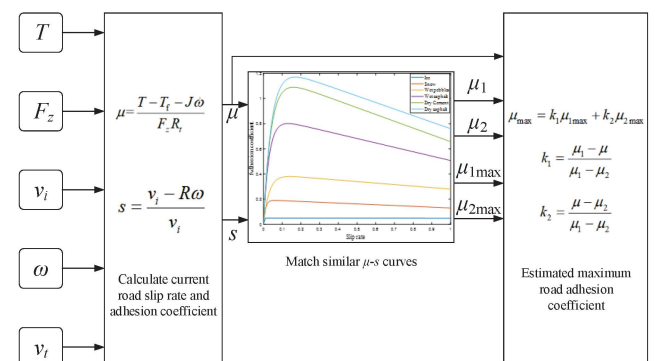


Fig. 3. Estimation model of road adhesion coefficient

B. Maximum deceleration

The ground braking force F_b and the adhesion force F_ϕ of the road surface during braking are constrained by the following equation:

$$F_b \leq F_\phi = G \mu_{\max} \quad (18)$$

where G is the gravity of the car, and μ_{\max} is the peak

adhesion coefficient of road surface.

The dynamic performance of the vehicle is not only constrained by the driving force, but also by the adhesion conditions between the tires and the ground. Therefore, the longitudinal acceleration of the vehicle is limited by the ground adhesion, and the following relationship is present:

$$a_d \leq \mu_{\max} g \quad (19)$$

where a_d is the braking deceleration, and g is the acceleration of gravity.

The vehicle enters the emergency obstacle avoidance condition when the vehicle achieves the safety distance threshold and obtains the maximum braking deceleration according to the estimated peak adhesion coefficient of the current driving surface to realize the active obstacle avoidance driving under the emergency obstacle avoidance condition.

C. Obstacle Avoidance Strategy in Emergency

The vehicle avoidance strategy should give priority to lateral steering to change lanes when both lateral steering avoidance and longitudinal braking avoidance are satisfied. Braking will affect the vehicles in the current lane, thus the traffic flow rate and road utilization are reduced. Therefore, vehicle steering avoidance should be given priority, and vehicle steering avoidance needs to consider the impact on other vehicles after vehicle steering. The decision logic of active obstacle avoidance is established in this paper, as shown in Fig. 4.

The comparison of the two obstacle avoidance modes in Fig. 4 is divided into two cases.

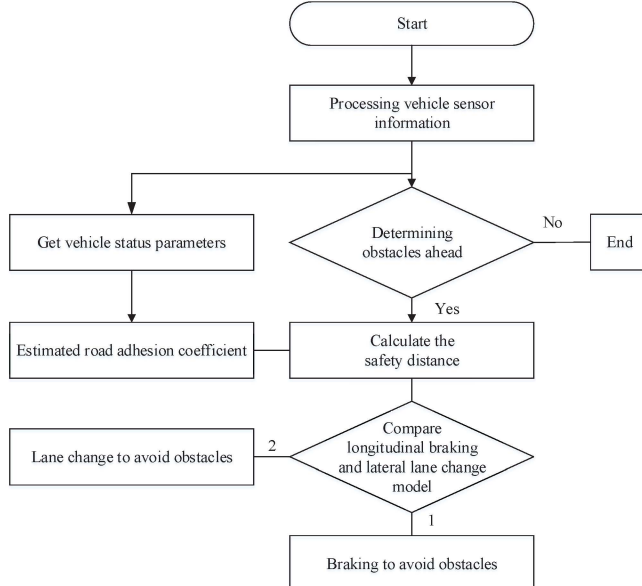


Fig. 4. The logic of active obstacle avoidance

Case1: $S_b < S_c$ or interference with vehicles in the target lane after a vehicle lane change.

$S_b < S_c$ means that the braking distance of the vehicle is less than the lane change distance. The vehicle can not complete the lane change operation, which requires braking avoidance. In the case of lane change operation interferes with the target lane vehicles also can not change lane to

avoid obstacles.

Case2: $S_b > S_c$ or Vehicles do not interfere with vehicles in the target lane after changing lanes.

$S_b > S_c$ indicates that the braking distance of the vehicle is greater than the lane change distance, and the lane change operation can be performed. Before the lane change operation, it detects whether the surrounding vehicle spacing is in the safe lane change interval, and then carries out the lane change operation.

IV. SIMULATION

A simulation scenario is constructed with the longitudinal safety distance as the obstacle avoidance warning mechanism. The self-vehicle travels at a uniform speed of 80 km/s in the lane, and the preceding vehicle moves at a uniform speed of 80 km/s and decelerates at a deceleration speed of 80/10.8 m/s² at t=4 s. The vehicle reaches the safety distance threshold at t=6 s. As shown in Fig. 5, the safety distance threshold is 25 m at this point and the main vehicle starts braking at the maximum braking deceleration speed. The vehicle parameters and the distance between the two vehicles during braking are shown in Fig. 5 and Fig. 6, respectively. Fig. 5 shows that when the vehicle brakes to a standstill, the two-vehicle spacing S_f is 2.3 m, and the simulation results satisfy the obstacle avoidance strategy designed in this paper. In this paper, the median value of the driver reaction time interval is taken as the driver reaction time in the simulation, and the brake effective time is 0.5 s.

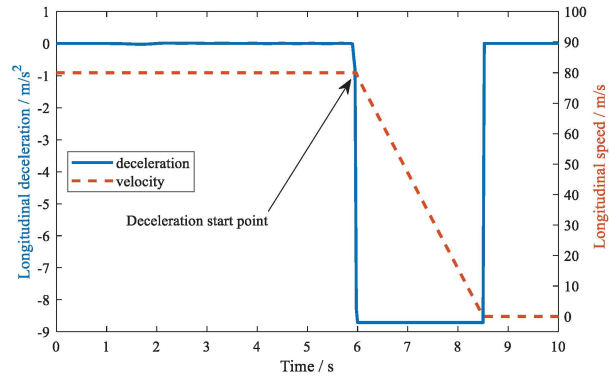


Fig. 5. Speed and deceleration of the self vehicle

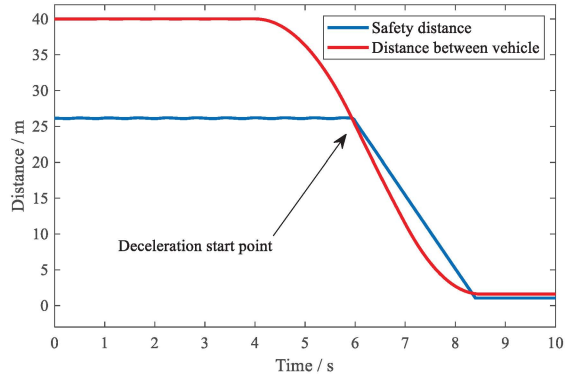


Fig. 6. Distance between the self vehicle and the preceding vehicle

The simulation scenario should be constructed by the lateral safety distance when the vehicle changes lanes. The self-vehicle travels at a uniform speed of 72 km/h on the road and maintains the longitudinal speed when changing lanes. The parameters of the other vehicles in the simulation

scenario are presented in Table I.

TABLE I. PARAMETERS OF OTHER VEHICLES IN THE SIMULATION

Vehicle number	X(m)	Y(m)	v_x (km/h)	a_x (m/s 2)
1	100	0	60	0
2	120	0	60	0
3	60	3.5	60	0
4	180	3.5	60	0

The vehicle parameters of the self-vehicle during the lane change are shown in Fig. 7.

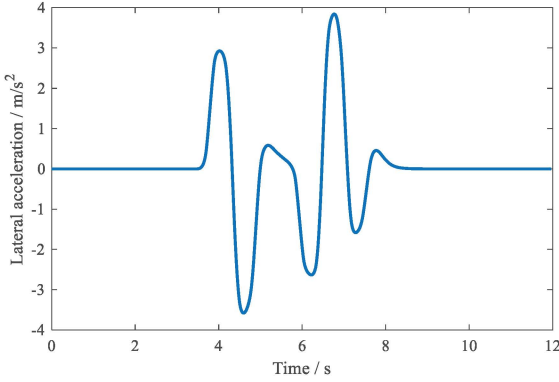


Fig. 7. Vehicle lateral acceleration

There is no obvious overshoot in lateral acceleration, and the convergence is relatively rapid after the lane change is completed, indicating that the attitude of the vehicle does not change drastically during the lane change, which has good stability.

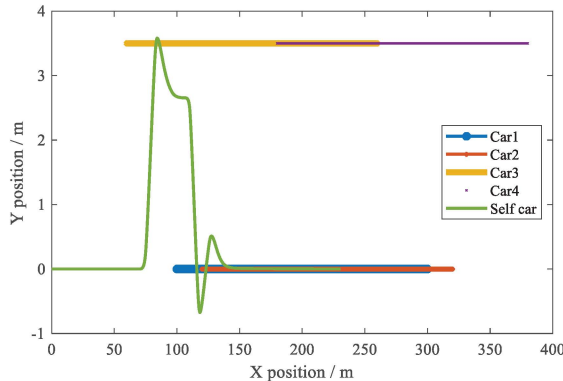


Fig. 8. Vehicle trajectory

The trajectory of the self vehicle and surrounding vehicles is shown in Fig. 8. According to the obstacle avoidance decision, the vehicle starts to change lane since $t=3.5$ s. After the first lane change is completed, the vehicle again detects whether there are obstacles around and calculates the safety distance of surrounding vehicles. According to the surrounding obstacle information, the main vehicle decides whether to enter the lane change state and changes lane to the initial lane at 5.8 s. In the case of complex road conditions and a lot of obstacle vehicles in the surrounding area, lateral lane change to avoid obstacles can

quickly get through the target road section.

V. CONCLUSION

This paper proposes an active obstacle avoidance strategy based on the transverse and longitudinal safety distance model. After analyzing the longitudinal safety distances for different states of motion of the preceding vehicle, a lateral safety distance interval combining the shortest lane change time and the longitudinal safety distance is constructed. In this interval, the lane-changing behavior of the vehicle will not cause interference to the vehicles in the target lane. The road adhesion coefficient is estimated and the maximum braking deceleration is calculated based on the vehicle sensor information. Simulation results show that the obstacle avoidance strategy established in this paper can effectively complete the active obstacle avoidance in both longitudinal and transverse directions, and the vehicle can make lane change to avoid obstacles and pass the target section quickly under the complex road environment.

REFERENCES

- [1] Al-Gabalawy, M. Hosny, N.S. & Aborisha, Ah.S, "Model predictive control for a basic adaptive cruise control," International Journal of Dynamics and Control, vol. 9, no. 3, pp. 1132-1143, 2020.
- [2] F. Farivar, M. Sayad Haghghi, A. Jolfaei and S. Wen, "On the Security of Networked Control Systems in Smart Vehicle and Its Adaptive Cruise Control," in IEEE Transactions on Intelligent Transportation Systems, vol. 22, no. 6, pp. 3824-3831, June 2021.
- [3] J. David, P. Brom, F. Starý, J. Bradáč and V. Dynybyl, "Application of Artificial Neural Networks to Streamline the Process of Adaptive Cruise Control," Sustainability, vol. 13, no. 8, 4572, 2021.
- [4] X. Zhang, Y. Huang and K. Guo, "Integrated Spacing Policy Considering Micro- and Macroscopic Characteristics," Automotive Innovation 2, pp. 102-109, 2019.
- [5] P. Seiler, B. Song and J. K. Hedrick . "Development of a Collision Avoidance System," SAE Technical Paper 980853, 1998.
- [6] B. Johan, "Adaptive Cruise Control and Driver Modeling," Lund University, 2001.
- [7] Y. Tian, Y. Lian, T. Zhang, C. Tang and S. Qi, "A Lateral Active Collision Avoidance System Based on Fuzzy-PID and Sliding Mode Control for Electric Vehicles," 2020 IEEE 9th Data Driven Control and Learning Systems Conference (DDCLS), 2020, pp. 438-442.
- [8] Q. Wu et al., "Research on Lane-Change Strategy With Real-Time Obstacle Avoidance Function," in IEEE Access, vol. 8, pp. 211255-211268, 2020.
- [9] Y. Cao, Z. Cao and Z. Guo, "Research on the control of EPS based on the change of road adhesion coefficient," 2016 International Conference on Advanced Mechatronic Systems (ICAMechS), 2016, pp. 362-367, 2016.
- [10] J. Wang, W. Tang, Y. Zhang and Y. Wang, "Study on the Estimation Method of the Forces on Vehicle Tires for ESC System," 2019 3rd Conference on Vehicle Control and Intelligence (CVCI), 2019, pp. 1-4, 2019.
- [11] B. Leng, D. Jin, L. Xiong, X. Yang, Z. Yu, "Estimation of tire-road peak adhesion coefficient for intelligent electric vehicles based on camera and tire dynamics information fusion," Mechanical Systems and Signal Processing, vol. 150, 107275, 2021.
- [12] N. Xu, Y. Huang, H. Askari and Z. Tang, "Tire Slip Angle Estimation Based on the Intelligent Tire Technology," in IEEE Transactions on Vehicular Technology, vol. 70, no. 3, pp. 2239-2249, March 2021.